1 Introduction

The surface of a glacier differs from its surroundings. The contrast may be small in winter when the landscape is totally covered by snow. However, in summer the differences can become very large. Those parts of a glacier that are not covered by debris have a relatively high albedo. As a consequence, less solar energy is absorbed. The temperature of the glacier surface cannot rise above melting point, so on warm days it is a sink of energy for the overlying air.

On warm summer days alpine valleys heat up considerably. Slope winds help to distribute the warm air generated at the valley walls that face the sun. This process is quite effective and the air in a valley is rapidly mixed (characteristic time scale: 15 minutes). Due to differential heating along the valley axis, an up-valley flow is normally established: the valley wind (Defant, 1949; Hoinkes, 1954). The layer of air involved is typically 1 km thick and blows up-valley. The valley wind brings heat to melting glaciers. One would expect valley winds to become weaker when they reach the glacierised part of a valley. In fact, the situation may become quite complex because glacier ice and walls of bare rock may be distributed rather irregularly.

At night the air is cooled and a mountain wind flows down the valley. It is much weaker and shallower than the valley wind, because turbulent exchange between surface and air is suppressed by the stable stratification.

Systematic investigations of the heat budget of a melting glacier did not start until after the second world war. Pioneering work was done by Ambach (1962). A series of other investigations followed (e.g. Björnsson, 1972; Hogg et al., 1982; Ishikawa et al., 1992), and these studies have given us basic insight into the nature of the energy budget on glaciers.

In more recent years glacio-meteorological experiments have been done in which the components of the surface energy flux were measured simultaneously at a large number of stations (Oerlemans and Vugts, 1993; Greuell et al., 1997; Oerlemans et al., 1999). Large data sets have been obtained, providing insight into altitudinal gradients of meteorological quantities.

During the experiment on the Pasterze, Austria (Greuell et al., 1997; Van den Broeke, 1997), about 200 ascents were made with a cable balloon from the glacier. The sensor mounted on the balloon measures wind speed, wind direction, pressure, humidity and temperature. Graphs from a single ascent made on a day with fair weather illustrates the type of information that can be obtained (*figure 3.1*). The most outstanding feature is the sharp temperature increase just above the glacier surface, about 14 K within 20 m. The glacier wind has a maximum speed of about 5 m s^{-1}; the height of the wind maximum is just a few metres above the surface. At a height of about 80 m wind speed is low and the wind direction turns from down-glacier (~340°)

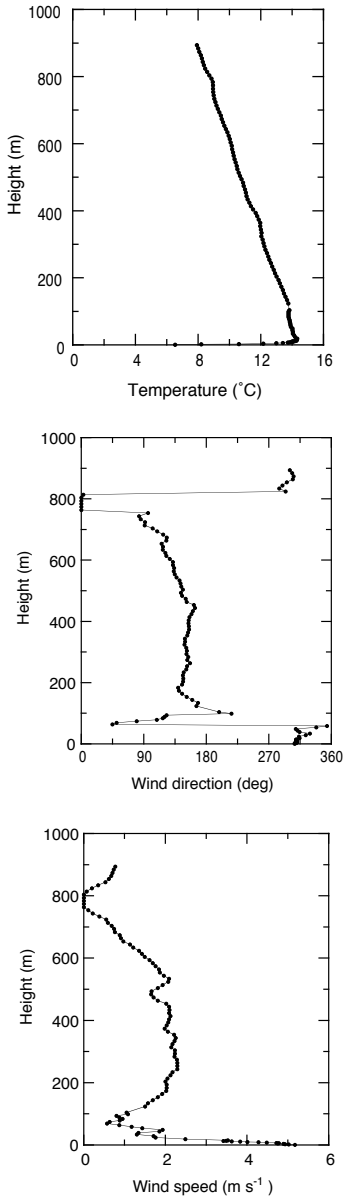

Figure 1. Structure of the atmosphere above the melting glacier tongue of Pasterze, Austria, as measured with a balloon. The ascent was made in fair weather on 23 July 1994, 16:25 local time. Note that the surface temperature is 0°C, implying a very large temperature gradient in the lower metres.

to up-glacier (~160°). Higher up the valley wind blows at a typical speed of 2 m s^{-1}. In the case shown the large-scale flow was very weak.

The observations reveal that in summer a circulation system, with a glacier wind driven by cooling of the air just above the glacier surface and a valley or synoptic-scale wind above, is present most of the time. This system is not restricted to valley glaciers but has also been observed over the melt zones of Vatnajökull (Iceland) and in West Greenland. The glacier wind may be an important mechanism for supplying heat to the melting glacier surface. Its structure and dynamics will therefore be discussed in some detail later.

For the melt process the surface energy budget is decisive. The mechanisms of heat transfer thought to be important for glaciers are shown in *figure 2*. The largest fluxes are the radiative fluxes, typically a few hundred Watts per square metre. A large part of the solar radiation reaching the glacier surface is reflected - more in the case of fresh snow, less in the case of old snow or bare ice, very little when the surface is covered by morainic material. Solar radiation penetrates into the snow and ice. In fact, the reflection as measured at the surface is the result of a complicated scattering process at the ice or snow crystals in the upper metres of the glacier. For long wave radiation the surface is very dense. It has an emissivity (and absorptivity) of about one. The amount of longwave radiation reflected by the surface is negligible - it is all absorbed. Incoming and outgoing longwave radiation compensate each other to a large degree. Normally the amount emitted by the surface is slightly larger (a few tens of Watts per metre squared) than the amount coming in from the atmosphere, making the net longwave balance negative. However, when the air is warm and humid, and clouds are present, the longwave balance may be positive.

The effect of clouds on the shortwave and longwave radiation budgets is of opposite sign. More clouds implies less shortwave radiation and more longwave radiation. The net effect depends on the surface albedo and on the cloud transmissivity (Ambach, 1974; Bintanja and Van den Broeke, 1996). For a high surface albedo (e.g. fresh snow) the net change in longwave radiation for a given increase in cloudiness is larger than the net change in the solar radiation. Consequenty, the net radiation balance increases. For lower albedo (e.g. ice) the solar radiation effect dominates and the net radiation budget decreases with cloudiness.

Turbulent exchange of heat and moisture can be quite significant, especially in winter (when the sun is low) or in summer when air temperature is high, as in the case shown in *figure 1*. The fluxes are in the direction of the gradients in the mean temperature and humidity profiles. When air temperature is above freezing point the sensible heat flux is always towards the surface. In such conditions the latent heat flux can go in both directions, depending on the

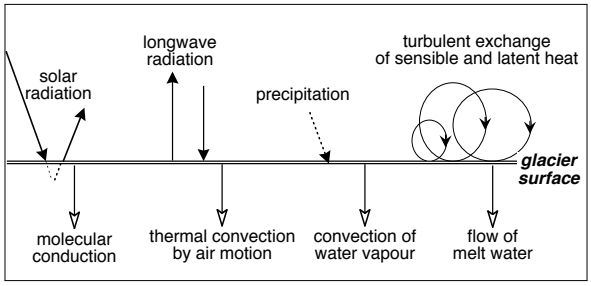

Figure 2. The most important processes determining the energy flux at the glacier-atmosphere interface and the thermal structure in the upper layer of the glacier.

humidity of the air. The saturation vapour pressure es for a melting glacier surface is 610.8 Pa. If an air mass has a temperature of 10°C, the gradient in vapour pressure and hence the vapour flux changes sign at a relative humidity of about 50%. At lower humidity evaporation cools the surface, at higher humidity condensation heats the surface.
The temperature of the precipitation may differ from the temperature at the surface. This implies that precipitation may add or remove heat from the existing snowpack or ice surface. However, the energy fluxes involved are small.
The fluxes inside the glacier are much smaller than those between atmosphere and glacier surface, except for the flow of melt water, which represents a latent heat flux. When glacier ice is at the surface molecular conduction is the only important process (note, however, that in the interior of cold glaciers conduction, frictional heating and advection due to ice motion have a similar order of magnitude).
In snow and firn, convection by air motion transports heat and water vapour. The fluxes are small but important for the metamorphosis of snow crystals. The vapour transport is determined mainly by the density of the snow and the temperature gradient. Fairly comprehensive models have been developed to describe the metamorphosis of snow in different climatic conditions; most of these models are connected with avalanche research.
For the study of the mass balance of temperate valley glaciers a description of the surface energy flux Ψ (in: W m^{-2}) is required. We write:

$$\Psi = Q(1-\alpha) + L_{in} + L_{out} + H_S + H_L + G \qquad (1.1)$$

Fluxes towards the glacier surface are defined as positive. L_{in} and L_{out} are incoming and outgoing longwave radiation, respectively. H_S is the turbulent sensible heat flux, H_L is the turbulent latent heat flux. G is the heat flux into or out of the glacier due to conduction and convection, and due to penetration of solar radiation. The first term on the right-hand side is the absorption of solar radiation. Q is the global radiation and a the albedo. Global radiation is defined as the amount of solar energy impinging on a horizontal surface coming in through a half-sphere. This implies that eq. (1.1) refers to a horizontal surface. The glacier surface is never horizontal and eq. (1.1) has to be modified if it is to be used for a real glacier.

2 Solar radiation - geometric factors

The real spectrum of solar radiation as measured outside the earth's atmosphere differs from the Planck function. During its path through the atmosphere the spectrum is further modified by scattering and absorption by air molecules, aerosols and clouds. The relevant quantity with respect to the surface energy flux is the spectrally

integrated solar radiation. The term albedo as used earlier is defined as the intensity of the spectrally integrated reflected solar radiation (upwards through a horizontal plane) divided by the intensity of the spectrally integrated global radiation (downwards through a horizontal plane).

The solar constant S is defined as the energy flux through a unit area perpendicular to the solar beam, at the mean earth-sun distance. Its value is 1368±3 W m^{-2}. At present, the earth-sun distance varies little over the year, because the eccentricity of the earth orbit around the sun (currently 0.0167) is small.

We now define the extra-terrestrial irradiance on a horizontal surface Q_E as

$$Q_E = S\left(\frac{\bar{r}}{r}\right)^2 \sin e \qquad (2.1)$$

Here e is the solar elevation, r the actual sun-earth distance and $\bar{r}$ its annual mean value. The solar elevation is given by

$$\sin e = \sin\phi \sin\delta + \cos\phi \cos\delta \cos h \qquad (2.2)$$

where ϕ is latitude, δ the solar declination and h the hour angle. The calculation of solar radiation for a given latitude at a given time of day is a standard procedure which will not be explained here (e.g. Walraven, 1978).

It is instructive to consider the effect of latitude on the extra-terrestrial irradiance, because it is one of the basic factors determining the length and intensity of the ablation season. Increasing latitude implies a smaller annual mean value, a larger seasonal amplitude and a smaller daily amplitude of Q_E. *Figure 3* shows how the daily mean value of Q_E, denoted by $Q_{E,day}$, varies through the year. In summer, values of $Q_{E,day}$ change little with latitude. Furthermore the well-known features are seen: the double maximum in the equatorial regions and the polar night at high latitudes.

It should be noted that there is no simple relation between Q_E and global radiation. Because the mean solar elevation is less at higher latitudes, the apparent optical mass of the atmosphere is larger and absorption and reflection of solar radiation are stronger.

The seasonal cycle increases with latitude but the daily cycle decreases (*figure 4*). Nevertheless, it is only at very high latitudes that the daily cycle in Q_E becomes really small.

A number of steps are needed to relate Q_E to the solar radiation that may become available at a glacier surface. First of all there are local geometric factors like shading by mountains, and the slope and aspect of the surface and reflection from surrounding slopes (*figure 5*).

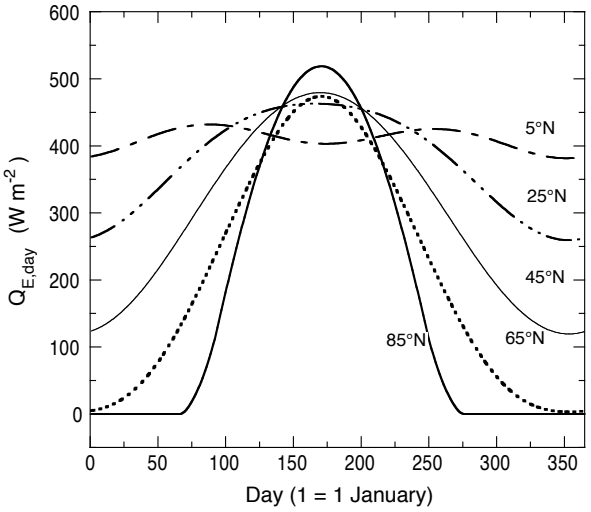

Figure 3. Daily mean values of the extra-terrestrial irradiance for a horizontal surface.

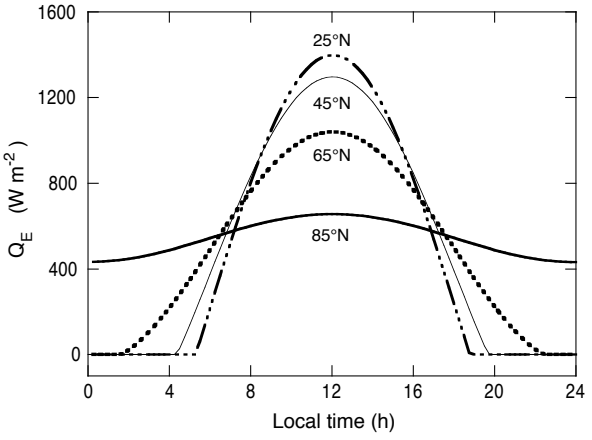

Figure 4. Extra-terrestrial irradiance for calendar day 181 at some selected latitudes.

To calculate the effect of geometry, the modification of the solar beam in the atmosphere has to be considered. Sophisticated methods have been devised to deal with this; the ultimate method for a valley with a complicated geometry in which scattering clouds are present is a Monte-Carlo technique which traces the path of millions of photons. However, simpler methods may sometimes be adequate for glacier applications (Oerlemans, 2001).

For many glaciers shading is a significant factor, or, put the other way round, glaciers tend to form in shaded places. Glaciers flowing into narrow deep valleys away from the sun can penetrate to much lower altitudes.

Figure 6 shows an example for day 202 at a latitude of 45°N. The attenuation of the solar radiation in the atmosphere was not taken into account. The shading angle is 25° and the slope of the surface is 10° to the north. Clearly, a considerable part of the extra-terrestrial irradiance does not reach the surface.

Figure 5. North-facing slopes of the Perschgletscher (a tributary of the Mortertaschgletscher, Switzerland)

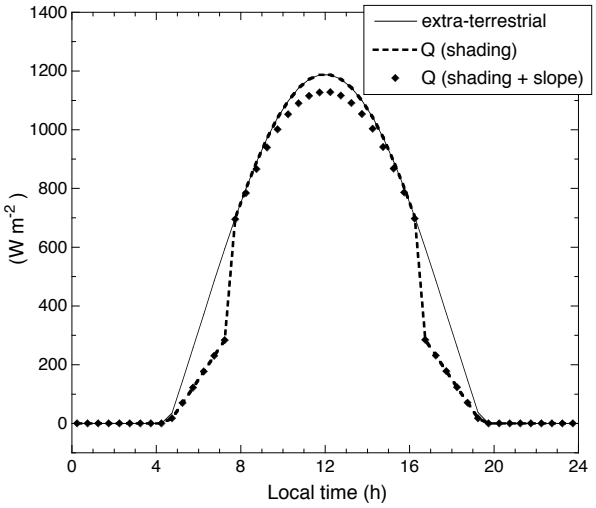

Figure 6. The effects of slope and shading for a cloudless day at 45°N. The shading angle is 25°. The surface slopes 10° to the north (Oerlemans, 2001).

3 Solar radiation - atmospheric effects

Scattering and absorption of solar radiation in the atmosphere, notably by clouds, now need to be considered as well. In the following discussion we will refer to transmissivities to describe the attenuation of the solar flux in the atmosphere:

$$Q = \tau_e \, Q_E = \tau_{cl} \, \tau_a \, \tau_g \, Q_E \qquad (1)$$

Here t_e is the total effective transmissivity, τ_{cl} the cloud transmissivity, τ_a the transmissivity due to absorption and scattering by air molecules, water vapour and aerosol. The geometric effects (shading, reflections from surrounding slopes) are represented by τ_g. Eq. (3.1) looks simple because the problems are hidden: the transmissivities are not independent. Geometric effects as discussed above depend on the cloud conditions and it is difficult to disentangle all the possible interactions. Nevertheless, to arrive at a workable approach that can be used in mass-balance models, eq. (3.1) is a useful starting point.

The theory of scattering and absorption of solar radiation in the atmosphere is well developed (e.g. Liou, 1980). Many algorithms have been constructed to calculate solar fluxes for a prescribed composition of the atmosphere. In general, the accuracy of calculations performed with such algorithms is limited by the quality of the input data, not by deficiencies in the radiative transfer theory.

Clouds form a particularly difficult aspect. In recent years, the application of satellite data has led to substantial

progress in the quantification of cloud distribution and cloud physical properties. However, glacio-meteorology has not benefitted much. The detection of clouds over highly reflective surface from satellite data is much more difficult. For ice sheets and ice caps some information can be obtained, but there is a lack of data about valley glaciers. Weather satellites are not really helpful because the scale is too small.

From these considerations it will be clear that ground measurements of the solar flux on glaciers are very useful. For shorter periods of time these are available from the studies mentioned earlier. However, longer time series are also needed; these can only be obtained from automatic weather stations. Automatic weather stations are indeed used on glaciers and ice sheets. Most of them are in the accumulation zones, very few in the ablation zones. The reason is clear: ablation zones are difficult to work in because access is difficult and melt rates are high. Stations should be able to stay in place even when 5 to 10 m of ice melts away in one year.

Figure 7 shows a record of global radiation from the station at the Morteratschgletscher (*figure 8*) (Oerlemans and Knap, 1998). The station is located on the lowest part of the glacier, about 500 m from the glacier front, at an altitude of 2100 m. The surrounding mountains are typically 3000 - 4000 m high. The highest mountains are to the south and to the west, providing efficient shading with shading angles of up to 40°. In the example shown the 4th of April was a cloudy day, the period 5-7 had few clouds and on the 8th conditions were variable. On this day multiple reflections between clouds, snow-covered valley walls and glacier surface led to a peak value (half-hourly mean) that is comparable to the extra-terrestrial irradiance.

Figure 10 shows a 1-year record of daily mean global radiation (Q_d) from the Morteratsch station. Due to the high degree of shading the annual mean global radiation is only 49% of the extra-terrestrial irradiance. There is a strong day-to-day variation in Q_d, which is due almost entirely to varying cloud conditions. For the summer half year it is possible to draw an envelope that more or less marks the clear-sky global radiation (= $\tau_a\ \tau_g\ Q_E$, dashed line in the figure). For the winter and early spring this is not possible because in those periods there is a strong interaction between clouds and the snow-covered valley walls.

Averaged over the period 1 April - 30 September 1996, the mean value of Q is 203 W m^{-2}, and the estimated clear-sky global radiation is 290 W m^{-2}. In this case therefore clouds have reduced the global radiation by 30%. However, cloud observations are not available. To establish a more explicit relation between Q and cloudiness, more detailed

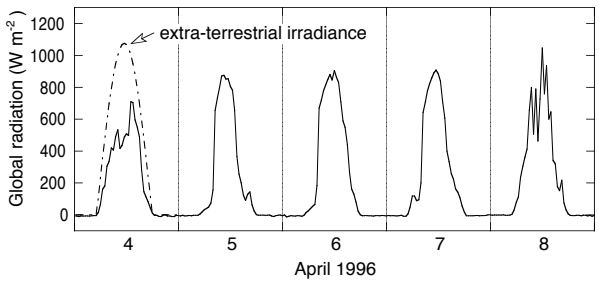

Figure 7. A record of global radiation from the automatic weather station on the tongue of the Morteratschgletscher, Switzerland.

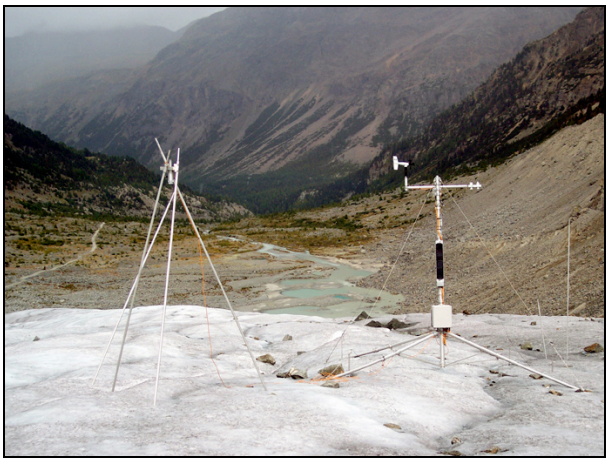

Figure 8. The IMAU automatic weather station on the tongue of the Morteratschgletscher.

measurements have been analysed. It appears that the relation between cloud transmissivity and cloudiness can be described well by a second order polynomial:

$$\tau_{cl} = 1 - c_1 n - c_2 n^2 \qquad (3.2)$$

Here n is the fractional cloudiness. In principle c_1 and c_2 are constants for a specific location, but a dependence on altitude has some times been included.

Figure 9 shows some examples for Alpine terrain and for the Greenland ice sheet. From this picture it is quite clear that clouds on the Greenland ice sheet are optically thinner, especially at higher elevation. There is little effect of such clouds up to a fractional cloud cover of 0.3.

It is clouds which cause most of the temporal variability of global radiation, but other processes in the atmosphere like scattering and absorption by air molecules and aerosol contribute significantly to the overall depletion of solar radiation. The various constituents all have different scattering functions and absorption spectra, but a treatment of these goes beyond the scope of this course. Instead we take a further look at data.

A survey of how global radiation in summer increases with altitude is presented in *figure 11*. First of all it is interesting to note that the values for the mean global radiation measured in high summer on the Pasterze and in Greenland are similar (260 - 300 W m-2). Over the entire period of measurements (22 May - 31 August) the values from Vatnajökull are much smaller. When the period 15 June -

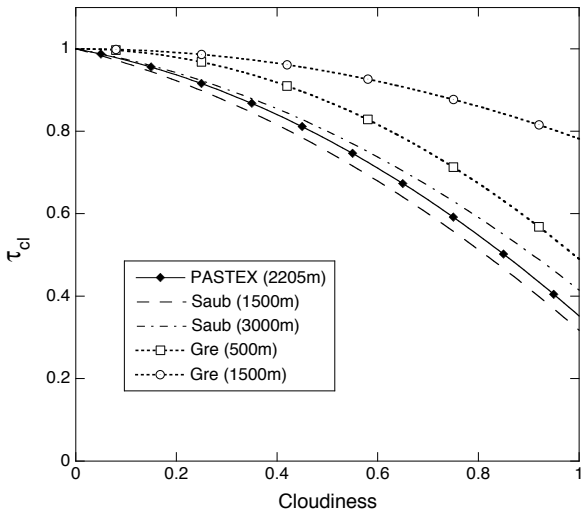

Figure 9. Parameterisation of cloud transmissivity based on measurements on the Pasterze glacier in Austria (PASTEX, Greuell et al., 1997), on a collection of measurements in the Alps from different sites (Sauberer, 1955) and on measurements made in the ablation zone of the west Greenland ice sheet (Gre, Oerlemans and Vugts, 1993).

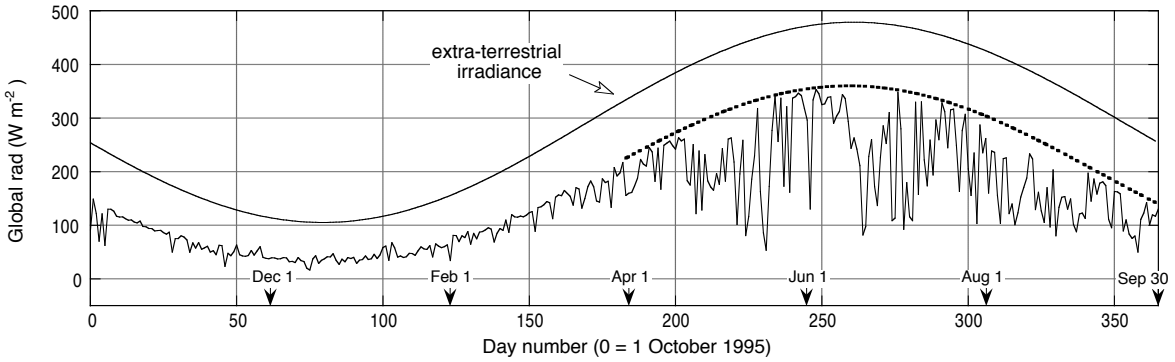

Figure 10. A one-year record of daily mean global radiation from the Morteratsch AWS. The dashed line is an attempt to eastimate the clear-sky global radiation.

31 July is considered, a better comparison with the other data can be made. Nevertheless, the amount of global radiation in the lower reaches of Vatnajökull is relatively small.

First of all it is interesting to note that the values for the mean global radiation measured in high summer on the Pasterze and in Greenland are rather similar (260 - 300 W m^{-2}). Over the entire period of measurements (22 May-31 August) the values from Vatnajökull are much smaller. When the period 15 June-31 July is considered, a better comparison with the other data can be made. Nevertheless, the amount of global radiation in the lower reaches of Vatnajökull is relatively small.

A more detailed analysis of the data reveals that the differences seen are again due mainly to differences in cloud amount and cloud type. This applies to the characteristic values of global radiation as well as to their altitudinal gradients. In general, clouds over the central western part of the Greenland ice sheet are optically thin and high, and the cloudiness is relatively small. This is in sharp contrast with Vatnajökull where low clouds are present most of the time and lead to a very strong increase in global radiation with altitude.

The data point from the Pasterze marked * is an outlier caused by intense reflection from surrounding slopes and should not be used to determine an altitudinal gradient. The variability for the Vatnajökull data is larger than for the other two data sets. This is due to the fact that the stations were widely spaced, covering the entire ice cap (area: 8400 km^2).

Clearly, all data sets show a consistent positive gradient in the global radiation with altitude.

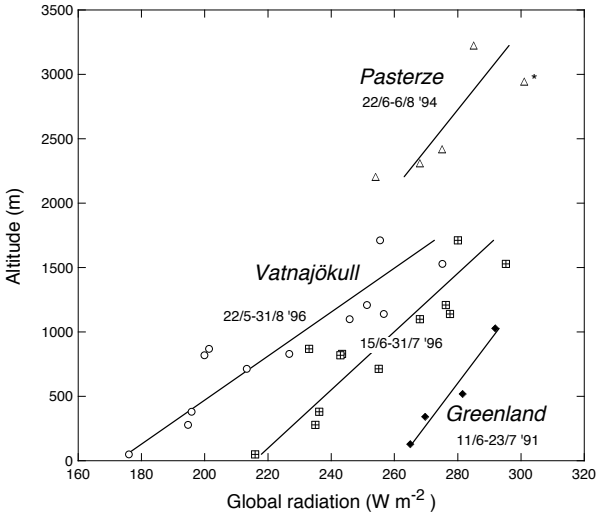

Figure 11. Parameterisation of cloud transmissivity based on measurements on the Pasterze glacier in Austria (PASTEX, Greuell et al., 1997), on a collection of measurements in the Alps from different sites (Sauberer, 1955) and on measurements made in the ablation zone of the west Greenland ice sheet (Gre, Oerlemans and Vugts, 1993).

4 The surface albedo

Later we will see that solar radiation contributes most to the surface energy flux when melting occurs. This makes the surface albedo a particular important quantity deserving a great deal of attention. Albedo depends in a complicated way on crystal structure, surface morphology, dust and soot concentrations, morainic material, the presence of liquid water in veins and at the surface, solar elevation, cloudiness, etc. It appears to be a fairly hopeless task to quantify and model all these factors, but maybe the most important can be captured by looking carefully at the sparse data available.

The spatial and temporal variation of the albedo is large. This can be observed when crossing glaciers on foot, but is far clearer when one looks at satellite images of sufficiently

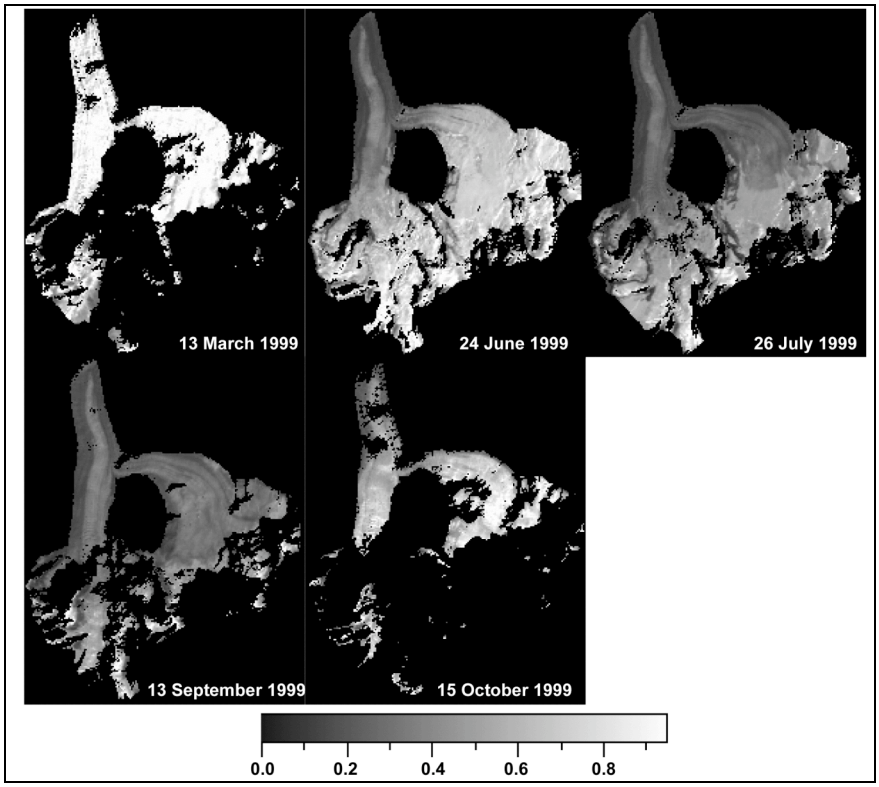

Figure 12. The evolution of the albedo of the Morteratschgletscher derived from Landsat Thematic Mapper images (Klok and Oerlemans, 2003).

high resolution. *Figure 12* shows an example of how the albedo of a valley glacier evolves in time. The maps have were derived from Landat images (Klok and Oerlemans, 2003). The Landsat Thematic Mapper images are quite useful because the resolution (30 m) is good enough to map valley glaciers. The disadvantage is the long repeat time of 16 days. Since cloud-free images are required to determine the surface albedo from the satellite measurements, one is lucky if one gets several useful scenes within a melt season. In the summer of 1999 this was the case for some glacierised parts of the Alps. For the Morteratsch-gletscher five cloud-free images were available. The transition from a fully snow-covered glacier in spring to a glacier which relatively low albedo at the end of the summer is clearly seen. In October fresh snow fell on the glacier. However, the sun was low then and many parts of the glacier were in the shade (black in the image). For these parts the albedo cannot be derived.

We go on to look at more data. *Figure 13* shows a 1-year record of daily albedo from the weather station on the Morteratschgletscher . Snow depth is also shown, because it explains most of the albedo variations seen. The snow

depth was measured with an ultrasonic ranger (20 kHz) which sampled every 3 hours. It is clear that a small amount of fresh snow brings the albedo up to about 0.8. Many peaks in the albedo record can be linked to the snow depth record. In the course of spring the snow albedo tends to decrease more or less steadily until day 215, when 20 cm of snow fell.

The ice albedo is between 0.3 and 0.4 but increases during the last part of the ablation season.

A scatter plot of all half-hourly values of global and reflected radiation for this year shows a clustering of data points (*figure 14*). The points are aligned along a characteristic albedo of snow (~0.7) and a characteristic albedo of ice (~0.3). For some data points the reflected radiation exceeds the global radiation. These are the cases where the upward-facing sensor is (partly) covered by snow.

The annual albedo is 0.491 (the annual mean albedo is 0.555). Therefore at this site about half of the global radiation is actually absorbed by the glacier surface.

Recalling that the global radiation was 49% of the extra-terrestrial irradiance we conclude that only 24% of the solar radiation available at the top of the atmosphere is absorbed at the glacier surface.

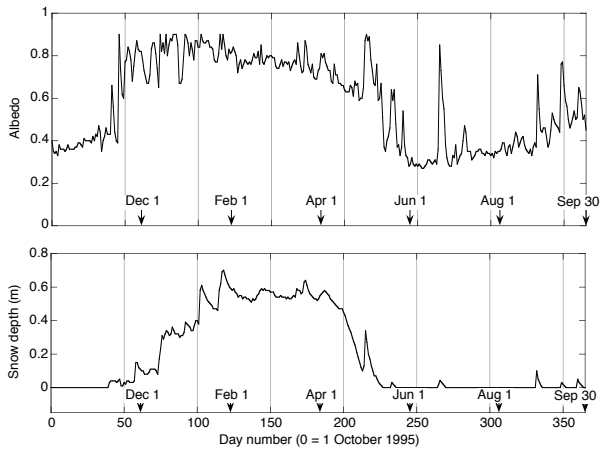

Figure 13. A 1-year record of daily albedo from the AWS on the Morteratschgletscher. The snow depth was measured with an ultrasonic ranger (Oerlemans and Knap, 1998).

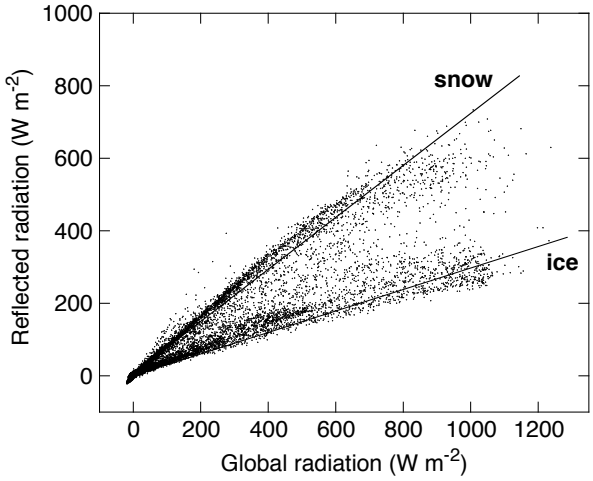

Figure 14. One year of half-hourly values from the AWS on the Morteratschgletscher (Oerlemans and Knap, 1998).

5 Longwave radiation

As for shortwave radiation, the basic theory for calculating the longwave fluxes for given profiles of atmospheric composition, clouds and temperature is well developed. However, these profiles are seldom measured over glaciers! One can either assume standard profiles for most of the constituents and run advanced radiation codes or one can rely on simpler schemes that have been calibrated carefully against measurements.

Do such measurements exist for glaciers? Yes they do, but the data sets are limited. Measurements of longwave radiation have been made as part of most of the energy-balance studies mentioned earlier. Unfortunately, it is not easy to measure the upward and downward longwave fluxes accurately. The performance of the instruments depends on temperature fluctuations and in particular on the presence of droplets, rime or snow on the sensor. Nevertheless, some useful data exist for a few sites in summer.

To illustrate the relation of longwave radiation to other meteorological quantities, *figure 15* shows a record of longwave radiation with global radiation, relative humidity and air temperature. Again, the data are from the station on

the Morteratschgletscher. Although cloud observations are not available, a good impression can be obtained from the global radiation. We can be fairly sure that 3rd August was a cloudy day, 4th and 5th were partly cloudy, and 6th and 7th were bright days with no or very little cloud cover.

The outgoing longwave radiation is rather constant as one would expect when the surface is melting all the time. However, the flux is larger than that emitted by a black body at melting point, which is 315 W m^{-2}. The difference can be attributed to the fact that the sensor is 3.5 m above the surface. The air between the surface and the sensor has a temperature of typically 10°C and will make a positive contribution to the upward flux measured at 3.5 m.

The incoming longwave radiation shows more pronounced variations. In the first half of the record this is due first of all to cloudiness and humidity, whereas in the second half it is mainly a response to air temperature.

The net radiation is shown at the bottom of the figure. The global radiation clearly dominates the picture, in spite of the fact that part of it (~30%, not shown) is reflected. However, from this we cannot conclude that longwave radiation is insignificant. It forms a larger part of the energy budget in autumn and winter. In addition, we should realise that air temperature has a direct effect on the longwave radiation - not on the solar radiation. Longwave radiation thus plays an important role as far as the climate sensitivity of glacier melting is concerned.

In simple parameterisations of longwave radiation the basic assumption is that the contributions from the cloudy and non-cloudy parts of the sky can be separated (Kimball et al., 1982; Oerlemans and Hoogendoorn, 1989):

$$I_{in} = \left[\varepsilon_{cs}\,(1-n^p) + \varepsilon_{cl}\,n^p\right]\sigma T_s^4 \qquad (5.1)$$

Here ε_{cs} and ε_{cl} are the characteristic emissivities for clear-sky and fully cloudy conditions, respectively. Cloudiness is denoted by n and air temperature at 2 m by T_a. The exponent p is determined by fitting eq. (5.1) to measurements. The clear-sky emissivity depends on the concentration of greenhouse gases, all lumped together in a constant, and on vapour pressure e_a and temperature (both at 2 m):

$$\varepsilon_{cs} = 0.23 + b\left(\frac{e_a}{T_a}\right)^{1/8} \qquad (5.2)$$

Again, the parameter b has to be found by fitting eq. (5.2) to observations. Greuell et al. (1997) found as best parameter values for the Pasterze experiment: p = 2, ε_{cl} =

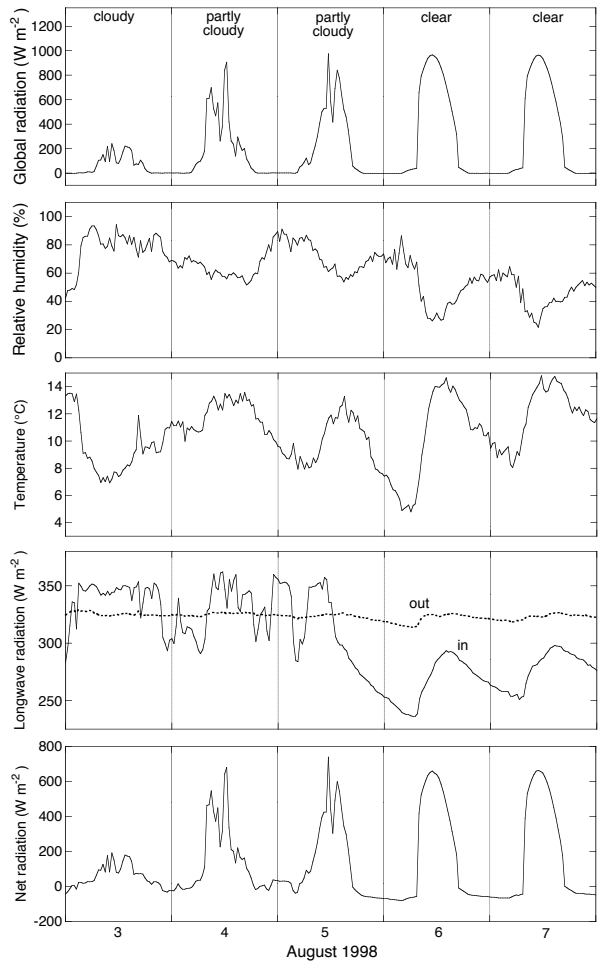

Figure 15. Measurements from the AWS on the Morteratschgletscher, showing incoming and outgoing longwave radiation in relation to other meteorological quantities (half-hourly mean values). Note the difference in vertical scale on the radiation panels.

0.976, b = 0.475 (on the glacier tongue), b = 0.407 (in the accumulation area).

The parameterisation described above has to be used with care, especially with regard to input data. When temperature and humidity are measured at a different height the parameter values have to be changed. In practice it is preferable to reduce the measurements to the level for which the parameterisation was derived, but from a general point of view it would be better to express the incoming longwave flux in terms of temperature and humidity at a greater height above the surface, preferably above the inversion. However, very few data of this kind are available.

Another weakness of eq. (5.1) is that the cloud contribution to Iin does not depend on cloud height and/or temperature. From a physical point of view this would be more desirable. However, in practical calculations these quantities are generally not known. By fitting eq. (5.1) to data the effect of cloud base temperature is absorbed in the cloud emissivity. When the cloud base is higher, the value of ε_{cl} will be slightly lower because of a lower temperature at the cloud base.

References and further reading

Ambach W. (1963): Untersuchungen zum Energieumsatz in der Ablationszone des Grönlandischen Inlandeises. *Meddelelser om Grønland* **174** (4), 311 pp.

Ambach W. (1974): The influence of cloudiness on the net radiation balance of a snow surface with high albedo. *Journal of Glaciology* **13**, 73-84.

Bintanja R. and M.R. van den Broeke (1996): The influence of clouds on the radiation budget of ice and snow surfaces in Antarctica and Greenland in summer. *International Journal of Climatology* **16**, 1281-1296.

Björnsson H. (1972): Bægisarjökull, North Iceland. Results of glaciological investigations 1967-1968, Part II. The energy balance. Jökull 22, 44-59.

Defant F. (1949): Zur Theorie der Hangwinde, nebst Bemerkungen zur Theorie der Berg- und Talwinde. *Archiv für Meteorologie, Geophysik und Bioklimatologie* **A1**, 421-450.

Greuell W., W.H. Knap and P.C. Smeets (1997): Elevational changes in meteorological variables along a midlatitude glacier during summer. *Journal of Geophysical Research* **102** (D22), 25941-25954.

Hoinkes H. (1954): Beiträge zur Kenntnis des Gletscher-windes. *Archiv für Meteorologie, Geophysik und Bioklimatologie* **B6**, 36-53.

Hogg I.G.G., J.G. Paren and R.J. Timmis (1982): Summer heat and ice balances on Hodges Glacier, South Georgia, Falkland Islands Dependencies. *Journal of Glaciology* **28**, 221-238.

Ishikawa N., I.F. Owens and A.P. Sturman (1992): Heat balance characteristics during fine periods on the lower parts of the Franz Josef Glacier, South Westland, New Zealand. *International Journal of Climatology* **12**, 397-410.

Kimball B.A., S.B. Idso and J.K. Aase (1982): A model of thermal radiation from partly cloudy and overcast skies. *Water Resources Research* **18**, 931-936.

Klok E.J., J.W. Greuell and J. Oerlemans (2003): Temporal and spatial variation of the surface albedo of the Morteratschgletscher, Switzerland, as derived from 12 Landsat images. *Journal of Glaciology* **49** (167), 491-502.

Konzelmann T., R.S.W. van de Wal, W. Greuell, R. Bintanja, E.A.C. Henneken and A. Abe-Ouchi (1994): Parameterization of global and longwave incoming radiation for the Greenland Ice Sheet. *Global and Planetary Change* **9**, 143-164.

Liou K. (1980): *Radiation in the atmosphere*. Academic Press, Orlando, 392 pp.

Oerlemans J. (2001): *Glaciers and climatic change*. Balkema/ Francis & Taylor.

Oerlemans J., H. Björnsson, M. Kuhn, F. Obleitner, F. Palsson, P. Smeets, H.F. Vugts and J. de Wolde (1999): Glacio-meteorological investigations on Vatnajökull, Iceland, summer 1996: an overview. *Boundary-Layer Meteorology* **92**, 3-26.

Oerlemans J. and N. C. Hoogendoorn (1989): Mass balance gradients and climatic change. *Journal of Glaciology* **35**, 399-405.

Oerlemans J. and W.H. Knap (1998): A 1 year record of global radiation and albedo in the ablation zone of Morteratschgletscher, Switzerland. *Journal of Glaciology* **44**, 231-238.

Oerlemans J. and H.F. Vugts (1993): A meteorological experiment in the melting zone of the Greenland ice sheet. *Bulletin of the American Meteorological Society*, 74, 355-365.

Sauberer S. (1955): Zur Abschätzung der Global-strahlung in verschiedenen Höhenstufen der Ostalpen. *Wetter und Leben* **7**, 22-29.

Walraven R. (1978): Calculating the position of the sun. *Solar Energy* **20**, 393-397.